PHYSICAL REVIEW B **91**, 121201(R) (2015)

Spin and photophysics of carbon-antisite vacancy defect in 4*H* silicon carbide: A potential quantum bit

Krisztián Szász,[1,2] Viktor Ivády,[1,3] Igor A. Abrikosov,[3,4,5] Erik Janzén,[3] Michel Bockstedte,[6,7,8] and Adam Gali[1,9,*]

[1]*Institute for Solid State Physics and Optics, Wigner Research Centre for Physics, Hungarian Academy of Sciences, P.O. Box 49, H-1525 Budapest, Hungary*

[2]*Institute of Physics, Loránd Eötvös University, Pázmány Péter sétány 1/A, H-1117 Budapest, Hungary*

[3]*Department of Physics, Chemistry, and Biology, Linköping University, SE-581 83 Linköping, Sweden*

[4]*Materials Modeling and Development Laboratory, National University of Science and Technology "MISIS", 119049 Moscow, Russia*

[5]*LOCOMAS Laboratory, Tomsk State University, 634050 Tomsk, Russia*

[6]*Lehrstuhl für Theoretische Festkörperphysik, Universität Erlangen-Nürnberg, Staudtstrasse 7 B2, D-91058 Erlangen, Germany*

[7]*FB Materialwissenschaften & Physik, Universität Salzburg, Hellbrunner Str. 34, A-5020 Salzburg, Austria*

[8]*European Theoretical Spectroscopy Facility, Spanish node, University of the Basque Country UPV/EHU, Avenida Tolosa 72, E-20018 Donostia/San Sebastián, Spain*

[9]*Department of Atomic Physics, Budapest University of Technology and Economics, Budafoki út 8., H-1111, Budapest, Hungary*

(Received 7 August 2014; revised manuscript received 25 February 2015; published 16 March 2015)

Silicon carbide with engineered point defects is considered as very promising material for the next generation devices, with applications ranging from electronics and photonics to quantum computing. In this context, we investigate the spin physics of the carbon antisite-vacancy pair that in its positive charge state enables a single photon source. We find by hybrid density functional theory and many-body perturbation theory that the neutral defect possesses a high spin ground state in 4*H* silicon carbide and provide spin-resonance signatures for its experimental identification. Our results indicate the possibility for the coherent manipulation of the electron spin by optical excitation of this defect at telecom wavelengths, and suggest the defect as a candidate for an alternative solid state quantum bit.

DOI: 10.1103/PhysRevB.91.121201 PACS number(s): 78.67.Bf, 71.15.Qe, 73.22.−f

Dopants and intrinsic point defects in solids show a rich spin and photo physics. They are promising candidates for implementations of quantum bits for quantum computing [1,2] and single-photon light sources for quantum cryptography. A leading contender in solid-state quantum information processing is by now the negatively charged nitrogen-vacancy defect (NV center) in diamond [3] because of its unique magneto-optical properties, long spin coherence time (up to several milliseconds in ultrapure diamonds [4]) and ease of optical initialization and readout of spin state [5], even nondestructively [6,7]. The optical initialization and readout of the electron spin state is based on the robust optically detected magnetic resonance (ODMR) signal of the NV center. Yet, the notion of defect quantum bits is not limited to diamond and the NV center. Given the fascinating potential of the defect spin and photo physics it is pivotal to investigate other semicondcutor materials and defects in this direction.

The wide-band-gap SiC has got the capability to host other color centers acting as quantum bits [8–11]. Exploring SiC-hosted qubits with favorable spin and optical properties for integration with existing semiconductor and optics technologies is the subject of intense research activity. Gali *et al.* proposed earlier that the high-spin divacancy defect in silicon carbide (SiC) with similar electronic structure as the NV center in diamond could be utilized as a solid state quantum bit [8]. In a recent breakthrough work by Koehl *et al.* [12], a coherent manipulation of divacancy and related defect spins in 4*H* polytype of SiC has been demonstrated. Also coupled spins of the negatively charged Si-vacancy have been investigated in this respect [11,13,14]. Recent milestones on the way towards the robust SiC-based quantum information technology are the finding of a coherence time of the divacancy qubits on the order of ∼1 ms at low temperatures [15] and the operation of isolated Si-vacancy qubits at room temperature [16]. A single photon light source was also created with the positively charged carbon antisite-vacancy pair in 4*H* SiC [17]. This defect is the transform of the silicon vacancy [18–20]. Favorable spin and optical properties are related to a particular charge state. This brings about the notions of charge state control and the spin and photo physics of the very important carbon antisite-vacancy pair defect. Exploring these notions is the aim of our present investigations.

Employing density functional theory and many body perturbation theory, we show in this Rapid Communication that the neutral carbon antisite-vacancy pair (CAV) has a high-spin ground state ($S = 1$), and investigate the spin and photophysics of this defect. The finding of a metastable closed shell singlet is unexpected for a carbon vacancy-related defects and may be relevant for this class of defects. Towards the experimental identification of the neutral CAV pair via spin resonance experiments we calculate hyperfine parameters and zero-field splitting. Our results suggest that its spin may be coherently manipulated by optical excitation in *n*-type 4*H* SiC. The theoretical predictions for the neutral CAV defects in 4*H* SiC provide an additional target for researchers seeking for solid state single color centers for quantum information processes and metrology. The calculated zero-phonon lines of the optically excited state is around 1500 nm, which fits perfectly to the telecom wavelengths, that makes this qubit

*gali.adam@wigner.mta.hu

candidate very promising for integration of quantum optics devices with existing fiber optics technology.

The CAV defects in 4*H* SiC are modeled in a 576-atom supercell. The electronic structure is calculated using HSE06 hybrid functional [21,22] within density functional theory (DFT). With this technique, it is possible, in particular, to reproduce the experimental band gap of SiC and the charge transition levels in group-IV semiconductors within 0.1 eV accuracy [23]. The adiabatic charge transition level, i.e., occupation level going from q to q' charge states is labeled as $(q|q')$. We apply a correction to the formation energies in the case of charged defects [24]. The zero-phonon line excitation energies are calculated by constrained-occupation DFT method (CDFT) which provides excellent results for NV center in diamond [25]. In our simulations, we apply VASP 5.3.3 plane wave code [26] within projector-augmentation-wave-method (PAW) [27,28]. We utilize the standard PAW potentials and a convergent plane wave cutoff of 420 eV. In the calculation of the hyperfine constants, the spin polarization of the core electrons is also taken into account [29]. We calculate the zero-field splitting due to electron spin–electron spin dipole-dipole interactions as described in Ref. [30].

Going beyond the hybrid density functional theory, quasiparticle (QP) energies and excitation spectra are obtained within many body perturbation theory in the G_0W_0 approach [31,32] and by solving the Bethe-Salpeter equation (BSE) [33] as implemented in VASP. The capability for the prediction of defect excitation spectra and the analysis of excitation thresholds was earlier demonstrated for the carbon vacancy in 4*H* SiC [34]. Accounting for the larger numerical effort of this approach, we employ a 288-atom supercell. For convergent response function calculations, a plane-wave cutoff of 100 eV and the inclusion of empty states up to 29 eV above the valence band maximum (E_V) are proven to be sufficient. Quasiparticle energies are obtained using the DFT-HSE06 Kohn-Sham states and energies as a starting point. Optical spectra are obtained by including excitonic effects via the BSE starting from the spin-polarized ground state.

The CAV defect is a complex of a carbon atom substituting a silicon atom in the lattice next to a carbon vacancy. It is a complimentary defect of silicon vacancy. A hop of a carbon neighbor of the silicon vacancy to the empty silicon lattice site transforms the latter into the CAV defect [18–20]. In 4*H* SiC, the CAV defects have four possible inequivalent configurations as shown in Fig. 1(a). Two of them are oriented parallel to the c axis (named parallel or hh and kk configurations), whereas the other two lie in the basal plane of the lattice (referred to as basal or hk and kh configurations). The parallel and basal configurations possess C_{3v} and C_{1h} symmetries, respectively [see Fig. 1(a)].

Let us start the analysis with the parallel configurations. Using group theory analysis and density functional theory calculations, Umeda *et al.* [35] have shown that a lower lying a_1 state, localized on the carbon antisite, and a higher lying double degenerate e state, localized on the carbon vacancy, form in the band gap [see Fig. 1(b)]. Also, a deep resonant a_1 state forms below E_V. The resonant and the localized states are filled by four electrons in the neutral charge state. Thus two electrons occupy the a_1 and e states in the band gap with either antiparallel ($S = 0$) or parallel spins ($S = 1$). In the former

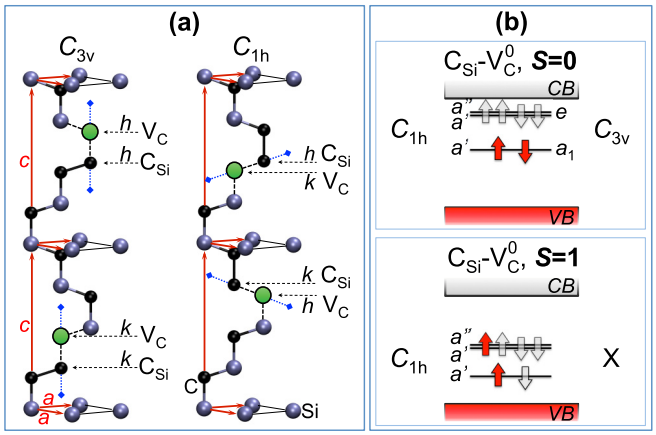

FIG. 1. (Color online) Schematic diagram of (a) the four possible configurations of carbon antisite-vacancy pair defects in 4*H* SiC and (b) the corresponding electronic structure in the singlet metastable and triplet ground states. The filled red and the outlined arrows indicate occupied and unoccupied single-particle states, respectively.

case, a closed shell singlet with a fully occupied a_1 state and an empty e state forms. Since there is a gap between the a_1 and e states one might consider the closed-shell singlet as the ground state.

In this Rapid Communication, we show that the $S = 1$ state should be also considered, where the a_1 and e states are occupied by a single electron each. From this Jahn-Teller unstable configuration, the defect reconstructs with a symmetry reduction to a configuration with C_{1h} symmetry. The reconstruction induces a splitting of the e state into a' and a'' states where the former can interact with the lower-lying a' state that derives from the a_1 state of the unreconstructed defect. We find that this interaction among these electron states, despite the energy gap between the initial a_1 and e, is so strong that the $S = 1$ state with C_{1h} symmetry becomes more stable than the closed-shell $S = 0$ state with C_{3v} symmetry. In the basal configurations, the starting symmetry is C_{1h} *per se*, which *ab ovo* splits the higher e state. Nevertheless, a similar process as for the parallel configurations takes place. The calculated energy difference between the singlet and triplet states are 0.30, 0.51, 0.46, and 0.55 eV for hh, kk, kh, and hk configurations, respectively. Thus, as a main result of our Rapid Communication, we identify with the neutral CAV a fundamental intrinsic defect in 4*H* SiC with a high spin ground state.

In the triplet state, two symmetrically inequivalent reconstructions of the vacancy occur due to the occupation of one of the two vacancy related e states with bonding and anti-bonding character between one pair of silicon atoms (in C_{1h} a'_{Si} and a''_{Si} respectively). For the energetically more favorable reconstruction, the triplet ground state has the electronic configuration $a'_C(1)\, a'_{Si}(1)\, a''_{Si}(0)$ [see Fig. 1(b)]. The electronic configuration $a'_C(1)\, a'_{Si}(0)\, a''_{Si}(1)$ leads to a distinct table reconstruction that is by 0.011, 0.011, 0.368, and 0.035 eV higher in energy for hh, kk, kh, and hk complexes, respectively. In the kh structure, this reconstruction has relatively high energy because of the unfavorable local geometry. For all CAV configurations, both triplet reconstructions are energetically more favorable than

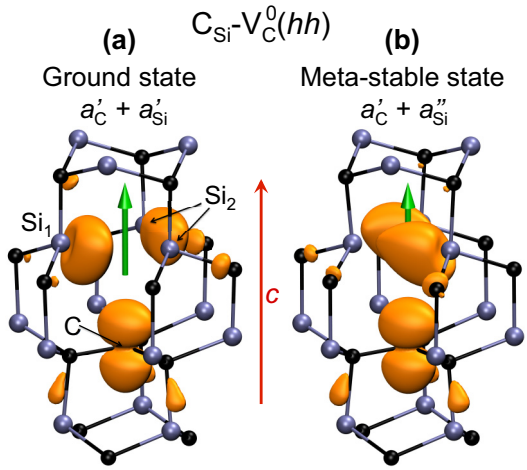

FIG. 2. (Color online) Isovalue surface of the spin density and the direction of the spin quantization (green arrows) in the (a) ground-state configuration and (b) metastable configuration of the neutral carbon anti-site vacancy pair at *hh* lattice configuration. In both cases, the isosurface value of 0.04 was chosen.

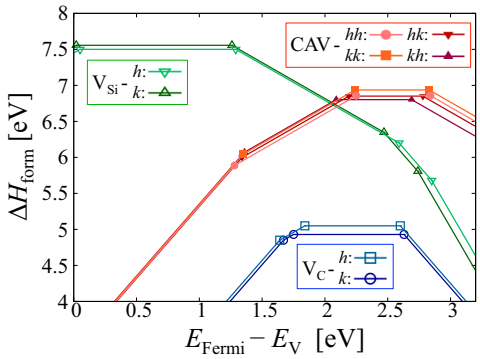

FIG. 3. (Color online) The calculated HSE06 formation energies (ΔH_{form}) of the carbon antisite-vacancy pair (CAV), the Si-vacancy (V_{Si}), and the C-vacancy (V_C) defects in 4*H*-SiC as a function of the Fermi-level (E_{Fermi}) with respect to the valence band maximum (E_V) in carbon-rich limit. For every defect, the symmetrically inequivalent configurations are depicted separately. The data related to V_C were taken from Refs. [38,39].

the singlet state and go along with large local structural reconstruction. For instance, in the triplet ground state of *hh* complex we found a distance of 2.71 Å between the symmetrically equivalent Si atoms, marked as Si_2 in Fig. 2, and distances of 3.03 Å between the Si atom, located on the mirror plain of C_{1h} symmetry and marked as Si_1 in Fig. 2, and the Si_2 atoms. In the metastable state we found 3.12 and 2.81 Å for these distances, respectively. The Jahn-Teller energy, i.e., the energy difference between the restricted C_{3v} configuration of the triplet state of the *hh* complex and its distorted C_{1h} reconstruction amounts to ∼0.3 eV. It is an upper bound for pseudo rotations of the complex between the symmetry equivalent C_{1h} ground states or metastable states. The large Jahn-Teller energy and the considerable distortion indicate a static Jahn-Teller effect.

The doping conditions at which the neutral CAV defect is stable can be obtained from an analysis of the defect formation energy as a function of the Fermi level position. It is shown in carbon-rich limit in Fig. 3. The result clearly shows that neutral CAV defects (zero charge state in the plots) are stable in *n*-type 4*H* SiC. On the other hand, it is well known that the CAV defect is only metastable with respect to a transformation into a Si vacancy in *n*-type 4*H* SiC (see Fig. 3). Nevertheless, once CAV defect is created a barrier energy of 2.4 eV is needed to convert it to a Si vacancy [19]. Indeed, simultaneous formation of CAV and Si-vacancy defects was detected in electron irradiated 4*H* SiC samples after 600 °C anneal for 1 hour [17]. The formation energy of CAV defects are comparable to those of C-vacancies in *p*-type 4*H* SiC, and may play an important role in *p*-type SiC devices (see Fig. 3). Indeed, our calculated (2+|+) and (+|0) levels at around $E_V + (1.28–1.36)$ eV and $+(2.09–2.25)$ eV, respectively, are very close to the recently detected deep level transient spectroscopy (DLTS) and minority carrier transient spectroscopy (MCTS) signals at $E_V + 1.56 \pm 0.2$ eV (HK_4) and $E_V + 2.26 \pm 0.1$ eV (EM_1) in *p*-type annealed SiC samples [36]. According to our previous results, the so-called AB photoluminescence lines [37] are associated with the positively charged CAV defects [17]. The single positively charged CAV defects can act as an ultrabright single photon-source that emits red light. The single-color centers can be formed by low-dose electron irradiation and annealing steps in high-purity semi-insulating (HPSI) 4*H* SiC [17]. Similarly, neutral CAV defects may be engineered for single defect measurements either in *n*-type 4*H* SiC or in HPSI SiC close to the surface, which may exhibit the appropriate band bending to stabilize the neutral charge state of CAV defects.

In view of the relevance of the CAV for qubit applications, let us analyze the ground state in more detail. The spin density distributions for the $S = 1$ neutral CAV defects in the ground and metastable configurations are depicted in Fig. 2. The unpaired electrons are both localized on the carbon antisite and the vacancy parts of the defect. The spin density is mostly found on carbon antisite resulting in large hyperfine coupling when C_{Si} is an ^{13}C isotope with $I = 1/2$ nuclei spin. Large hyperfine coupling can be found on the Si dangling bonds too when they constitute of ^{29}Si isotopes with $I = 1/2$ [40]. Larger than 1 MHz hyperfine signals can be found up to the fourth shell around the defect center that might be utilized to make entanglement between the electron spin and nuclei spins of ^{13}C or ^{29}Si. The $S = 1$ electron spin in anisotropic crystal field leads to zero-field splitting. As the symmetry of the defects is low three different principal values of the electron spin–electron spin zero-field tensor appear. The calculated values of the splitting parameter *D* and *E* are ranging from −2.22 to −2.16 GHz and from −90 to −210 MHz, respectively, among the ground states of symmetrically inequivalent configurations. The sign of *D* indicates that the $m_S = \pm 1$ substates have the deepest energy levels. In all configurations, the direction of the spin quantization is approximately parallel to the axis of the defect (see Fig. 2). In the metastable configurations, we observed similar properties of the zero-field interaction. We believe that these properties make CAV defect an important candidate for qubit application.

Next, the optical excitation of the CAV defects and the potential coherent manipulation of the spin states are

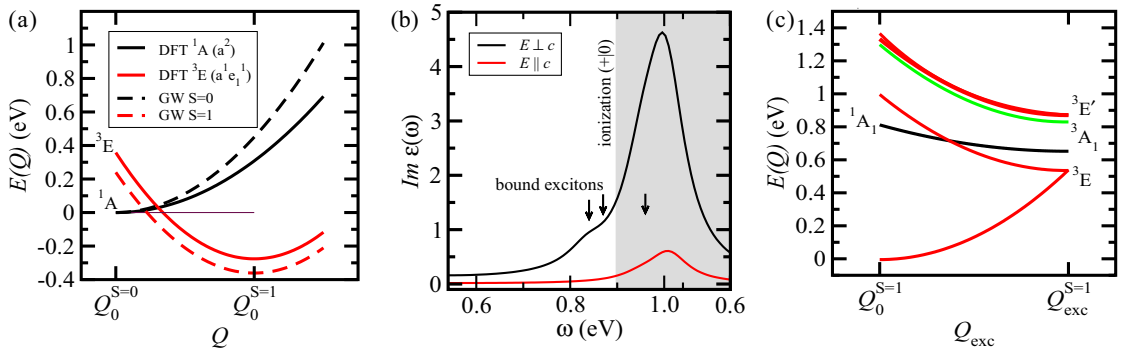

FIG. 4. (Color online) (a) PES of lowest singlet and triplet of the hh complex as obtained within G_0W_0 and DFT-HSE06 using the 288 atom cell. Q connects the singlet ($Q_0^{S=0}$) and the triplet ($Q_0^{S=1}$) ground-state (GS) configurations. (b) Absorption spectrum in the configuration of the excited triplet state (ES) as obtained from BSE calculations. Excitation occurs from the triplet GS configuration. The bound excitons are indicated along side with the ionization threshold. The first peak in this spectrum corresponds to the vertical emission energy. The polarization of the photons is indicated where c is the c-axis of $4H$ SiC parallel to the symmetry axis of the defect. We note that the bound exciton peak may be sharper; we used a broadening of ∼0.05 eV to produce a continuous absorption spectrum. (c) PES of the triplet states as obtained from BSE calculations (red and green lines). $Q_{\rm exc}$ connects the triplet GS and ES configurations ($Q_0^{S=1}$ and $Q_{\rm exc}^{S=1}$). The green line refers to the ^{3}A$_1$ state. The ^{1}A$_1$ singlet state (solid black line) was obtained from CDFT.

discussed. We performed G_0W_0 and BSE calculations for the hh complex. Using G_0W_0 calculations, the potential energy surface (PES) describing the singlet instability of the neutral complex can be obtained as a function the coordinate Q that linearly connects the singlet and triplet ground states geometries ($Q_0^{S=0}$ and $Q_0^{S=1}$, respectively) by adding electrons to the positively charge complex at the corresponding Q. We approximate the energy $E_S(Q)$ of the low/high spin state by the quasiparticle energy and DFT-HSE06 ground state of the positive CAV (CAV$^+$), i.e., $E_S(Q) \approx \varepsilon^{\rm QP}(Q) + E^{\rm DFT}_{\rm CAV^+}(Q)$. As shown in Fig. 4(a) the G_0W_0 confirms the findings obtained with DFT-HSE06, despite small numerical deviations.

We now turn to the optical excitation. Our result for the (+|0) occupation level of about 0.9 eV below the conduction-band minimum ($E_{\rm C}$) suggests fundamental excitations of the CAV complex in the near infrared region such as defect bound excitons. These excitons form via transitions from $a_{\rm C}'$ or $a_{\rm Si}'$ to extended states or defect resonances close to $E_{\rm C}$. Our BSE calculation yields bright exciton states that are located 0.1 eV below the vertical bound to free transition of the hh complex at $Q_0^{S=1}$. Subsequent geometrical relaxation in the excited state using the CDFT yields a zero phonon line (ZPL) of 0.84 eV (∼1476 nm). The excited electron is located in a defect resonance that derives from the antisite dangling bond and equal, small contributions from the Si dangling bonds of the vacancy. It is more delocalized than the hole in the defect state. Hence the relaxed geometry ($Q_{\rm exc}^{S=1}$) resembles the positively charged CAV and possesses C_{3v} symmetry. It differs from the singlet ground state $Q_0^{S=0}$ by an elongation of the C$_{\rm Si}$-Si distance of 4%. The two lowest bright excited triplets are ^{3}A$_1$ and ^{3}E′.

In Fig. 4(c), the potential energy surfaces of the triplet excited states (ES) are shown along the path that linearly connects the triplet ground state (GS) $Q_0^{S=1}$ and ES geometries $Q_{\rm exc}^{S=1}$. The surfaces were obtained by BSE calculations based on four geometries along the path and a fit to a harmonic form [41]. The adiabatic GS and the lowest triplet ES curves become degenerate ^{3}E triplets at $Q_{\rm exc}^{S=1}$. The latter curve derives from the metastable triplet shown in Fig. 2(b) and is essentially optically dark. The ^{3}A$_1$ state is indicated by the green line in Fig. 4(c). Also the closed-shell ^{1}A$_1$ singlet state as obtained from CDFT-calculations is shown. The excitation to the ^{3}E′ state induces in our CDFT calculations a slight distortion that lifts the orbital degeneracy. The distorted state possesses a similar ZPL as the transition to ^{3}A$_1$ state.

An almost identical result is obtained for the hh complex by CDFT simulating the occupation of orbitals taken from the solution of the BSE. The calculated excitation energy amounts to 0.81, 0.83, 0.95, and 0.86 eV for hh, kk, kh, and hk configurations, respectively. Note that the wave lengths of these ZPLs (∼1500 nm) are perfectly suitable for nowadays fiber optics technology.

The excited state triplets ^{3}A$_1$ and ^{3}E′ may couple nonradiatively to ground-state triplets via spin selective intersystem crossings mediated by spin-orbit and spin-spin interaction. It is difficult to predict open-shell singlet states besides the closed-shell singlet quantitatively at the moment. They are the subject of future studies. Nevertheless, such open-shell singlets that involve defect resonances exist in the energy range of the excited triplets ^{3}A$_1$ and ^{3}E′. At $Q_{\rm exc}^{S=1}$, the complex has C_{3v} symmetry. Based on group theory considerations, the triplet ^{3}A$_1$ and ^{3}E′ can for instance couple to intermediate ^{1}A$_1$ singlets by nonaxial spin-orbit interaction that flips the $m_S = \pm 1$ spin states of the triplet to $m_S = 0$ spin state, where m_S is the spin component of the spin quantization axis. From the intermediate singlet, the electron may decay both to $m_S = \pm 1$ or 0 spin states of the triplet ground state where the selection rules are much relaxed due to the low symmetry at $Q_0^{S=1}$. Nevertheless, this nonradiative process is spin-selective in the first step, thus spin-dependent contrast in the fluorescence rate is expected to appear upon appropriate photoexcitation of the defect. The spin-selective processes may compete with nonadiabatic transition between the ^{3}A$_1$, ^{3}E′, and ^{3}E energy surfaces, which would reduce the fluorescence yield and spin selectivity. Here an adequate assessment would require

yet unavailable knowledge of the full potential energy surfaces including the singlet states. However, all in all, our results suggest that a coherent manipulation of the neutral CAV spins should be feasible and should be investigated in experiments.

In summary, we studied the spin and photo physics of the carbon antisite-vacancy pair defect in 4H SiC by first-principles theory. We found that the neutral carbon antisite-vacancy pair defects exhibit a high spin ground state, and that they can be stable in n-type 4H SiC. Their spin and photo physics may enable an alternative and promising source for quantum information processing and metrology. Particularly, the calculated optical excitation wave lengths (∼1500 nm) suit perfectly to the fiber optics technology that provides a pave to scale-up these qubits into quantum network.

We acknowledge the support from the MTA Lendület program of Hungarian Academy of Sciences, the Knut & Alice Wallenberg Foundation "Isotopic Control for Ultimate Materials Properties", the Swedish Foundation for Strategic Research program SRL grant No. 10-0026, the SNIC 001/12-275 and SNIC 2013/1-331 supercomputer time at the National Supercomputer in Linköping and the HPC cluster of the RRZE of the University of Erlangen-Nürnberg. Use of the Center for Nanoscale Materials was supported by the US Department of Energy, Office of Science, Office of Basic Energy Sciences, under Contract No. DE-AC02-06CH11357. IAA is grateful to the Grant of Ministry of Education and Science of the Russian Federation (Grant No. 14.Y26.31.0005) and Tomsk State University Academic D. I. Mendeleev Fund Program.

[1] T. D. Ladd, F. Jelezko, R. Laflamme, Y. Nakamura, C. Monroe, and J. L. O'Brien, Nature (London) **464**, 45 (2010).

[2] D. D. Awschalom, L. C. Bassett, A. S. Dzurak, E. L. Hu, and J. R. Petta, Science **339**, 1174 (2013).

[3] L. du Preez, Ph.D. thesis, University of Witwatersrand, Johannesburg, 1965.

[4] G. Balasubramanian, P. Neumann, D. Twitchen, M. Markham, R. Kolesov, N. Mizuochi, J. Isoya, J. Achard, J. Beck, J. Tissler, V. Jacques, P. R. Hemmer, F. Jelezko, and J. Wrachtrup, Nat. Mater. **8**, 383 (2009).

[5] F. Jelezko and J. Wrachtrup, Phys. Status Solidi A **203**, 3207 (2006).

[6] B. B. Buckley, G. D. Fuchs, L. C. Bassett, and D. D. Awschalom, Science **330**, 1212 (2010).

[7] L. Robledo, L. Childress, H. Bernien, B. Hensen, P. F. A. Alkemade, and R. Hanson, Nature (London) **477**, 574 (2011).

[8] A. Gali, A. Gällström, N. Son, and E. Janzén, Mater. Sci. Forum **645–648**, 395 (2010).

[9] J. R. Weber, W. F. Koehl, J. B. Varley, A. Janotti, B. B. Buckley, C. G. Van de Walle, and D. D. Awschalom, Proc. Natl. Acad. Sci. USA **107**, 8513 (2010).

[10] A. Gali, Phys. Status Solidi B **248**, 1337 (2011).

[11] A. Gali, J. Mat. Res. **27**, 897 (2012).

[12] W. F. Koehl, B. B. Buckley, F. J. Heremans, G. Calusine, and D. D. Awschalom, Nature (London) **479**, 84 (2011).

[13] V. A. Soltamov, A. A. Soltamova, P. G. Baranov, and I. I. Proskuryakov, Phys. Rev. Lett. **108**, 226402 (2012).

[14] H. Kraus, V. A. Soltamov, D. Riedel, S. Väth, F. Fuchs, A. Sperlich, P. G. Baranov, V. Dyakonov, and G. V. Astakhov, Nat. Phys. **10**, 157 (2014).

[15] D. J. Christle, A. L. Falk, P. Andrich, P. V. Klimov, J. U. Hassan, N. T. Son, E. Janzén, T. Ohshima, and D. D. Awschalom, Nat. Mater. **14**, 160 (2015).

[16] M. Widmann, S.-Y. Lee, T. Rendler, N. Tien Son, H. Fedder, S. Paik, L. Yang, N. Zhao, S. Yang, I. Booker, A. Denisenko, M. Jamali, S. A. Momenzadeh, I. Gerhardt, T. Ohshima, A. Gali, E. Janzén, and J. Wrachtrup, Nat. Mater. **14**, 164 (2015).

[17] S. Castelletto, B. C. Johnson, V. Ivády, N. Stavrias, T. Umeda, A. Gali, and T. Ohshima, Nat. Mater. **13**, 151 (2014).

[18] E. Rauls, T. Lingner, Z. Hajnal, S. Greulich-Weber, T. Frauenheim, and J.-M. Spaeth, Phys. Status Solidi B **217**, r1 (2000).

[19] M. Bockstedte, A. Mattausch, and O. Pankratov, Phys. Rev. B **68**, 205201 (2003).

[20] T. Umeda, N. T. Son, J. Isoya, E. Janzén, T. Ohshima, N. Morishita, H. Itoh, A. Gali, and M. Bockstedte, Phys. Rev. Lett. **96**, 145501 (2006).

[21] J. Heyd, G. E. Scuseria, and M. Ernzerhof, J. Chem. Phys. **118**, 8207 (2003).

[22] A. V. Krukau, O. A. Vydrov, A. F. Izmaylov, and G. E. Scuseria, J. Chem. Phys. **125**, 224106 (2006).

[23] P. Deák, B. Aradi, T. Frauenheim, E. Janzén, and A. Gali, Phys. Rev. B **81**, 153203 (2010).

[24] C. Freysoldt, J. Neugebauer, and C. G. Van de Walle, Phys. Rev. Lett. **102**, 016402 (2009).

[25] A. Gali, Phys. Rev. B **80**, 241204 (2009).

[26] G. Kresse and J. Furthmüller, Phys. Rev. B **54**, 11169 (1996).

[27] P. E. Blöchl, Phys. Rev. B **50**, 17953 (1994).

[28] P. E. Blöchl, Phys. Rev. B **62**, 6158 (2000).

[29] K. Szász, T. Hornos, M. Marsman, and A. Gali, Phys. Rev. B **88**, 075202 (2013).

[30] A. L. Falk, P. V. Klimov, B. B. Buckley, V. Ivády, I. A. Abrikosov, G. Calusine, W. F. Koehl, A. Gali, and D. D. Awschalom, Phys. Rev. Lett. **112**, 187601 (2014).

[31] L. Hedin, Phys. Rev. **139**, A796 (1965).

[32] L. Hedin and S. Lindqvist, *Solid State Physics: Advances in Research and Application*, edited by F. Seitz, D. Turnbull, and H. Eherenreich (Academic, New York, 1969), Vol. 23, p. 1.

[33] M. Rohlfing and S. G. Louie, Phys. Rev. B **62**, 4927 (2000).

[34] M. Bockstedte, A. Marini, O. Pankratov, and A. Rubio, Phys. Rev. Lett. **105**, 026401 (2010).

[35] T. Umeda, J. Ishoya, T. Ohshima, N. Morishita, H. Itoh, and A. Gali, Phys. Rev. B **75**, 245202 (2007).

[36] G. Alfieri and T. Kimoto, Mater. Sci. Forum **778–780**, 269 (2014).

[37] J. W. Steeds, Phys. Rev. B **80**, 245202 (2009).

[38] T. Hornos, A. Gali, and B. G. Svensson, Mater. Sci. Forum **679–680**, 261 (2011).

[39] X. T. Trinh, K. Szász, T. Hornos, K. Kawahara, J. Suda, T. Kimoto, A. Gali, E. Janzén, and N. T. Son, Phys. Rev. B **88**, 235209 (2013).

[40] See Supplemental Material at http://link.aps.org/supplemental/10.1103/PhysRevB.91.121201 for calculated hyperfine tensors.

[41] Spin polarization of the ground state at the geometry $Q_{\rm exc}^{S=1}$ with C_{3v} leads to an artificial splitting of the degenerate ^{3}E and ^{3}E′ states within the BSE approach. We corrected for this error by removing the splitting via a manual shift of the potential curves.